

Detection and analysis of *Spartina alterniflora* in Chongming East Beach using Sentinel-2 imagery and image texture features

Xinyu Mei¹, Zhongbiao Chen^{1*}, Runxia Sun¹, Yijun He¹

¹ School of Marine Sciences, Nanjing University of Information Science and Technology, Nanjing 210044, China

Received 24 April 2024; accepted 12 September 2024

© Chinese Society for Oceanography and Springer-Verlag GmbH Germany, part of Springer Nature 2025

Abstract

Spartina alterniflora is now listed among the world's 100 most dangerous invasive species, severely affecting the ecological balance of coastal wetlands. Remote sensing technologies based on deep learning enable large-scale monitoring of *Spartina alterniflora*, but they require large datasets and have poor interpretability. A new method is proposed to detect *Spartina alterniflora* from Sentinel-2 imagery. Firstly, to get the high canopy cover and dense community characteristics of *Spartina alterniflora*, multi-dimensional shallow features are extracted from the imagery. Secondly, to detect different objects from satellite imagery, index features are extracted, and the statistical features of the Gray-Level Co-occurrence Matrix (GLCM) are derived using principal component analysis. Then, ensemble learning methods, including random forest, extreme gradient boosting, and light gradient boosting machine models, are employed for image classification. Meanwhile, Recursive Feature Elimination with Cross-Validation (RFECV) is used to select the best feature subset. Finally, to enhance the interpretability of the models, the best features are utilized to classify multi-temporal images and SHapley Additive exPlanations (SHAP) is combined with these classifications to explain the model prediction process. The method is validated by using Sentinel-2 imageries and previous observations of *Spartina alterniflora* in Chongming Island, it is found that the model combining image texture features such as GLCM covariance can significantly improve the detection accuracy of *Spartina alterniflora* by about 8% compared with the model without image texture features. Through multiple model comparisons and feature selection via RFECV, the selected model and eight features demonstrated good classification accuracy when applied to data from different time periods, proving that feature reduction can effectively enhance model generalization. Additionally, visualizing model decisions using SHAP revealed that the image texture feature component_1_GLCMVariance is particularly important for identifying each land cover type.

Key words texture features, Recursive Feature Elimination with Cross-Validation (RFECV), SHapley Additive exPlanations (SHAP), Sentinel-2 time-series imagery, multi-model comparison

Citation Mei Xinyu, Chen Zhongbiao, Sun Runxia, He Yijun. 2025. Detection and analysis of *Spartina alterniflora* in Chongming East Beach using Sentinel-2 imagery and image texture features. Acta Oceanologica Sinica, 44(2): 80–90, doi: 10.1007/s13131-024-2394-8

1 Introduction

Wetlands are renowned as the “kidney of the Earth” and a “treasure trove for humanity”, possessing some of the strongest self-purification capabilities among natural ecosystems, with estuarine tidal flats having the highest ecological service value per unit area (Costanza et al.,

1997). In recent years, the wetlands at the Changjiang River (Yangtze River) Estuary (Yangtze River) have been greatly troubled by the invasive species *Spartina alterniflora*, posing a significant threat to native plants like reeds and *Scirpus mariqueter*. Since the introduction of *Spartina alterniflora* to the Changjiang River Estuary in 1980, its distribution area had expanded to 6 200 hectares

Foundation item: The National Key Research and Development Program of China under contract No. 2023YFC3008204; the National Natural Science Foundation of China under contract Nos 41977302 and 42476217.

*Corresponding author, E-mail: chenzhongbiao@nuist.edu.cn

http://www.aosocean.com
E-mail: ocean2@hyxb.org.cn

by 2015, rapidly encroaching upon the habitat of native plants and causing significant impacts on coastal wetland ecosystems (Xu et al., 2018). Therefore, understanding the spatial and temporal distribution of different vegetation types in wetlands and grasping the competitive relationships between invasive and native vegetation is of great significance for the restoration and protection of wetland ecosystems. The feasibility of using remote sensing imagery for *Spartina alterniflora* detection has been proven.

Feng et al. (2022) successfully classified the vegetation of the Momoge Wetland in Jilin using time-series Sentinel-1 and Sentinel-2 imageries combined with machine learning methods, providing a highly generalizable model for wetland vegetation classification. Ren et al. (2014) analyzed the variations of *Spartina alterniflora* using an Support Vector Machine (SVM) classifier and multi-temporal Landsat remote sensing imagery, alongside annual data on the Huanghe River's (Yellow River's) sediment load and meteorological data. Gao et al. (2016) employed five image fusion algorithms to process Landsat imagery and used maximum likelihood, artificial neural networks, and SVM classifiers to classify wetlands on Chongming Island in Shanghai. Meng et al. (2021) proposed a phenology-based method for extracting *Spartina alterniflora* Loisel by using multi-year Landsat 8 Operational Land Imager (OLI) time series data from three major wetlands in the Changjiang River Delta region. Zhang et al. (2022) monitored the phenology of *Spartina alterniflora* in coastal areas of China using time-series Landsat 7/8 and Sentinel-2 imagery combined with three phenological detection methods, finding that with increasing latitude, the start of *Spartina alterniflora* phenology shifts later while the length of the phenological period shortens. Zhang et al. (2021) simulated the dynamic invasion and spread of *Spartina alterniflora* in the Huanghe River Delta from 2014 to 2018 by using cellular automaton models, showing that local plants have a minimal impact on the spread of the *Spartina alterniflora* population. Yao et al. (2017) proposed a method for distinguishing mixed zones of *Spartina alterniflora* and reeds based on their phenological differences and spectral characteristics, considering their distribution differences between coastal and inland and using measured profile observation data to determine spectral indices and thresholds. Mahdavi et al. (2018) discussed various remote sensing methods for wetland classification, highlighting the advantages and disadvantages of each, and concluded that the red edge and near-infrared bands are optimal optical bands for wetland delineation, while in Synthetic Aperture Radar (SAR) imagery, large incidence angles, short wavelengths, and horizontal transmit and vertical receive polarizations are most effective for detecting herbaceous wetlands. Zhang et al. (2017) enhanced remote sensing image classification accuracy by integrating directional measures with

Gray-Level Co-occurrence Matrix (GLCM) algorithms, while Lan and Liu (2018) optimized multi-scale parameters through GIS-domain knowledge integration; both approaches significantly improved classification performance while maintaining computational efficiency. Cui et al. (2023) proposed the MFVNet, a coastal wetland information extraction network that combines deep learning with vegetation indices, and demonstrated that this network achieved better information extraction results for coastal wetland vegetation types compared to deeper semantic segmentation networks like HRNet. However, the algorithms based on different deep learning methods require large datasets, high computing power, and poor interpretability.

Although remote sensing technology has been widely used for monitoring wetland vegetation, existing studies on remote sensing monitoring of *Spartina alterniflora* have limitations due to the complexity of coastal wetland ecosystems. These limitations mainly lie in the feature extraction from images and the choice of methods. Most studies have used deep learning to integrate vegetation index features for classification, with few utilizing image texture features for classification. However, in high-resolution remote sensing images, texture features contain more information than geometric and gray-level features, which is important for remote sensing image classification. Additionally, deep learning methods have high computational power requirements and poor interpretability. Therefore, this study selected the Dongtan area of Chongming Island as the study area, using multiple machine learning models and time-series remote sensing images to integrate image texture features and vegetation indices for the extraction study of *Spartina alterniflora*, and verified the role of image texture features in remote sensing monitoring and classification of *Spartina alterniflora*.

2 Material and methods

2.1 Study area

This study focuses on Chongming East Beach (Fig. 1). It extends from 31°26'00"N to 31°38'00"N in latitude and from 121°51'30"E to 122°03'00"E in longitude. This area is formed by sediment carried by the Changjiang River and was designated as an important international wetland in 2001. The primary salt marsh vegetation in the study area includes reeds, *Spartina alterniflora*, *Scirpus mariqueter*, among others. Dominant species include *Spartina alterniflora* and reeds, with *Spartina alterniflora* being more suitable for environments with high salt and low nitrogen levels. Additionally, in the northern part of the study area, from the embankment towards the river and sea, a distribution pattern has formed with pure reeds, a mixed zone of reeds and *Spartina alterniflora*, and pure *Spartina alterniflora*. The expansion trend of *Spartina alterniflora* and its competitive advantage in the mixed zone

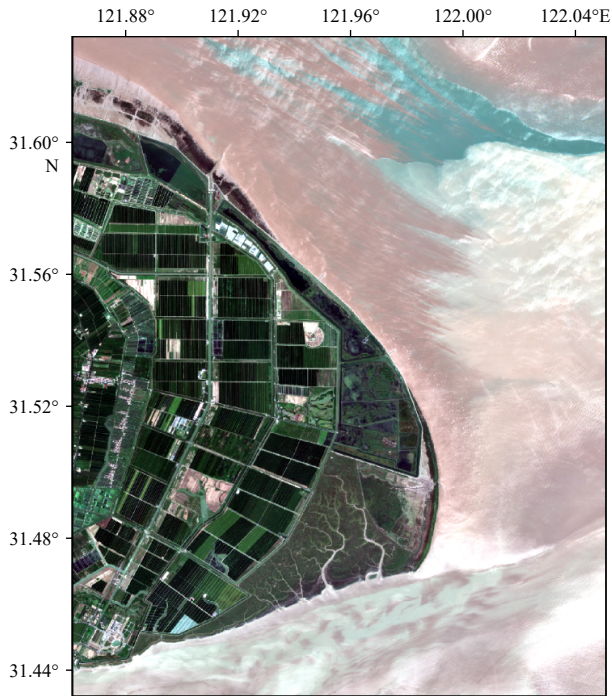


Fig. 1. Location of the study area.

are particularly evident (Jiang et al., 2009).

2.2 Data

2.2.1 Remote sensing imagery

In this study, the data utilized includes Sentinel-2 MultiSpectral Instrument (MSI) L2A imagery, which has high spatial resolutions and include 12 spectral bands. Through the Copernicus Data Space Ecosystem, a total of 90 images from 2020 to 2021 are selected, which are re-sampled to a spatial resolution of 10 m (Table 1).

2.2.2 Sample data

Based on previous relevant studies (Gao et al., 2016; Ding et al., 2015), index thresholds for classification are determined. The images are then classified using these thresholds, and finally, the accuracy of the classification is

Table 1. Spectral bands of Sentinel-2 MSI L2A (Segarra et al., 2020)

Band	Wavelength/nm	Resolution/m
B1: coastal aerosol	433–453	60
B2: blue	458–523	10
B3: green	543–578	10
B4: red	650–680	10
B5: vegetation red edge	698–713	20
B6: vegetation red edge	733–748	20
B7: vegetation red edge	773–793	20
B8: NIR	785–900	10
B8A: narrow NIR	855–875	20
B9: water vapour	935–955	60
B11: SWIR	1 565–1 655	20
B12: SWIR	2 100–2 280	20

Note: MSI, Multi-Spectral Instrument; NIR, Near-Infrared; SWIR, Shortwave Infrared.

validated by integrating high-resolution data from Google Earth. Use the Modified Normalized Difference Water Index (MNDWI) = 0.4 to distinguish between water and non-water bodies. Use the Normalized Difference Vegetation Index (NDVI) > 0.6 and the Difference Vegetation Index (DVI) > 0.33 to extract farmland areas. Use $B8 < 0.18$ to extract reed areas. Use $NDVI > 0.55$ and $DVI < 0.15$ to extract *Spartina alterniflora* areas. Use $0.101 < B4 < 0.125$ to extract reed-*Spartina alterniflora* mixed transition zones. Use the Ratio Vegetation Index (RVI) as a feature in subsequent research.

$$NDVI = \frac{B8 - B4}{B8 + B4}, \quad (1)$$

$$MNDWI = \frac{B3 - B11}{B3 + B11}, \quad (2)$$

$$RVI = \frac{B8}{B4}, \quad (3)$$

$$DVI = B8 - B4. \quad (4)$$

This process results in land cover interpretation images of the study area. Using the Sentinel Application Platform (SNAP), samples of various land cover types are selected, resulting in the selection of 160 sample points of land cover. Through stratified sampling, a training to validation sample ratio of 7 : 3 is employed, resulting in the following distribution of training and validation samples for each land cover type: 31 samples for farmland, 27 samples for reeds, 29 samples for *Spartina alterniflora*, 24 samples for the mixed zone of *Spartina alterniflora* and reeds (staggered bands), 33 samples for water bodies, and 30 samples for other land cover types (Table 2).

2.3 Methods

In this study, a framework is developed to extract *Spartina alterniflora* in the study area and assess its accuracy (Fig. 2). Within this framework, 20-dimensional features are first extracted from the remote sensing images. During feature extraction, considering the high degree of

Table 2. Training and validation data of different land cover types

Type	Label	Number of training samples	Number of validation samples
Farmland	1	22	9
Reed	2	19	8
<i>Spartina alterniflora</i>	3	20	9
Staggered bands	4	17	7
Water	5	23	10
Other (bare ground, building, <i>Scirpus</i>)	6	21	9

Note: Staggered stands for *Spartina alterniflora*-reed mixed staggered zone; type stands for land cover type.

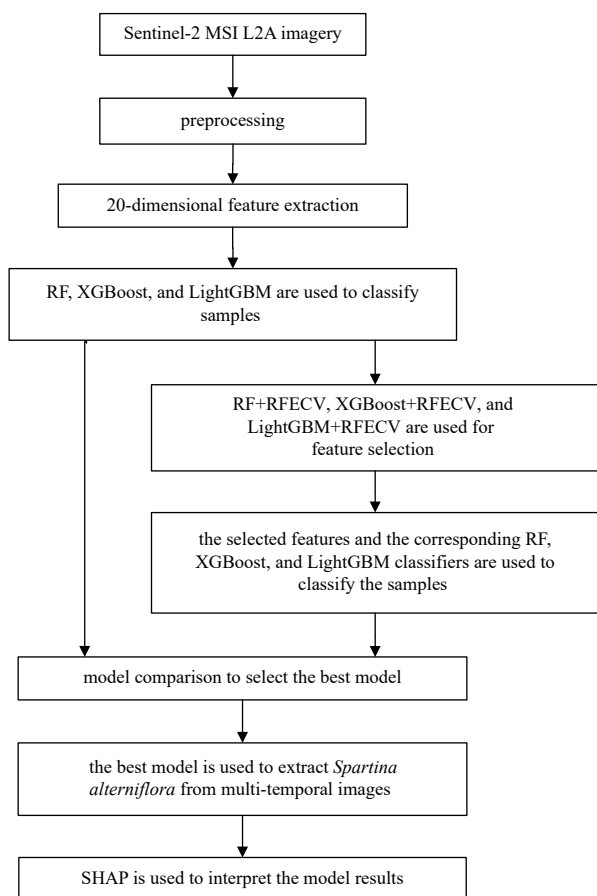


Fig. 2. Process framework of this study. MSI: Multi-Spectral Instrument; RF: Random Forest; XGBoost: eXtreme Gradient Boosting; LightGBM: Light Gradient-Boosting Machine; RFECV: Recursive Feature Elimination with Cross-Validation; SHAP: SHapley Additive exPlanations.

deformation and large scale variations of coastal wetland vegetation in remote sensing images, the Principal Component Analysis-Gray-Level Co-occurrence Matrix (PCA-GLCM) (Hall-Beyer, 2017) method is utilized for texture feature extraction among the 20-dimensional features. Related research has demonstrated that *Spartina alterniflora* in the coastal areas of the Changjiang River Estuary exhibits the best separability in September (Ouyang et al., 2013). Therefore, to enhance the separability between *Spartina alterniflora* and *Phragmites australis*, remote sensing images from September are selected to extract indices such as NDVI and RVI. Subsequently, the Random Forest (RF), eXtreme Gradient Boosting (XGBoost), and Light Gradient Boosting Machine (LightGBM) models are used to classify the samples.

Then, these three models are combined with Recursive Feature Elimination with Cross-Validation (RFECV) to construct RF+RFECV, XGBoost+RFECV, and LightGBM+RFECV models for feature selection, identifying the optimal feature combination for each model. Finally, the models with the optimal feature combinations are compared with the models using the 20-dimensional fea-

ture set, and the best model is selected to extract *Spartina alterniflora* in the study area.

2.3.1 Data preprocessing

Image processing mainly includes radiometric calibration, atmospheric correction, geometric correction, cropping, and resampling. Since Sentinel-2 MSI L2A data products have already undergone radiometric, atmospheric, and geometric corrections, only cropping and resampling of the images are required. In this study, Google Earth high resolution reality data is used to verify the accuracy of the threshold to distinguish land cover.

2.3.2 Multi-dimensional shallow feature extraction of images

In the study area, *Spartina alterniflora* is densely distributed, with a high canopy cover within the population (Zhu et al., 2019). Based on these characteristics, the following vegetation indices are selected: NDVI, RVI for vegetation, DVI sensitive to soil background changes for farmland areas, and MNDWI for water bodies. Additionally, several texture features from the first principal component of the image PCA-GLCM are chosen, including Contrast, Angular Second Moment (ASM), Entropy, and GLCM Variance. These features are called component_1_Contrast, component_1_ASM, component_1_Entropy, and component_1_GLCMVariance.

Combining these eight features with the original spectral bands, a fused feature set of 20-dimensions is used as input for classification purposes.

2.3.3 Machine learning models integrating shallow features

In order to reduce the cost of training the model and enhance the interpretability of the model, this study opts for ensemble learning algorithms that are more suitable for structured data and have lower computational demands. Firstly, Sentinel-2 remote sensing images have multispectral characteristics, with up to 13 bands, providing rich information for land cover classification. The identification of *Spartina alterniflora* relies on the combination of multiple bands. RF, XGBoost, and LightGBM perform well in handling high-dimensional data and can effectively utilize this band information to improve classification accuracy. Secondly, the spectral characteristics of *Spartina alterniflora* exhibit non-linear traits, such as its specific spectral reflectance being influenced by the interaction of multiple bands (Shao et al., 2024). RF and gradient-boosting-based models like XGBoost and LightGBM are adept at capturing these complex non-linear relationships, thereby enhancing the accuracy of the classification models. Lastly, *Spartina alterniflora* is a typical wetland plant, with specific characteristics in its spectral reflectance in the Near-Infrared (NIR) and Short-wave Infrared (SWIR) bands (Shu et al., 2019). These features are distinctly different from those of surrounding

vegetation and water bodies. Machine learning models, such as RF, XGBoost, and LightGBM, can effectively distinguish *Spartina alterniflora* from other species by analyzing these spectral characteristics. In addition, in this study, the longitude, latitude, and 20-dimensional features of the pixels contained in the sample region are extracted and organized into a table for training the model. And the prediction results of tree-based models on tabular data are still better than those of deep learning (Grinsztajn et al., 2022). Therefore, a tree-based model is selected for classification in this study. The GridSearchCV method with 10-fold cross-validation in scikit-learn adjusted the RF model, XGBoost model and LightGBM model.

(1) RF: The parameters selected for optimization include the following. The maximum depth of the tree is 30. And random sampling is conducted without playback. The minimum number of samples required at the leaf node is 1, and the minimum number of samples required to split an internal node is 2. A total of 100 decision trees are used in the model, and randomness in both sampling and bootstrap processes is controlled by setting a fixed seed value of 42.

(2) XGBoost: The parameters selected for optimization include the following. The maximum depth of the tree is set to 6. A random sample of 80% of features is selected when constructing each tree. The learning rate, which controls the step size of the iterative decision tree, is set to 0.2. The model includes 300 weak learners, and 100% of the data is used for each iteration.

(3) LightGBM: The parameters selected for optimization include the following. The maximum depth of the tree is 10. The learning rate, which controls the contribution of each tree in the gradient boosting algorithm, is set to 0.1. The model is trained with 500 estimators, and each tree contains 50 leaf nodes.

The application of models in this study is as follows. Based on the interpretation of ground object images, Region of Interest (ROI) samples for each type of ground object are drawn and the extracted features are integrated to construct RF, XGBoost, and LightGBM models for classifying the sample set. Hyperparameter optimization and cross-validation are performed using GridSearchCV to prevent overfitting and improve model accuracy. Subsequently, based on these three models, RFECV is used to construct RFECV+RF, RFECV+XGBoost, and RFECV+LightGBM models to select the best feature subset from the original feature set. Finally, the selected best feature subset and models are used to classify the remote sensing images of the study area, and the accuracy and interpretation are evaluated using SHapley Additive exPlanations (SHAP).

2.3.4 Feature selection

Due to the risk of overfitting, in order to enhance the model's generalization ability, improve its performance on new data, and eliminate redundancy between features, the most representative features are selected from the 20

dimensional features for subsequent classification. Based on this, RFECV is chosen for feature selection to find the optimal feature combination (Chen and Jeong, 2007).

Since RFECV is a heuristic search algorithm in the wrapper method based on model scores and feature importance, it is sensitive to the model used. Therefore, we respectively use RF+RFECV, XGBoost+RFECV, and LightGBM+RFECV for feature selection to find the optimal feature combination for each corresponding model. Finally, we select the best feature combination and model by considering both model accuracy and resource consumption.

2.3.5 Model accuracy evaluation

To validate the classification results of the imagery, this study adopts the confusion matrix as an evaluation metric, including, Producer Accuracy (PA) and User Accuracy (UA), and Overall Accuracy (OA). The calculation formulas are as follows:

$$PA = \frac{c_{ii}}{c_{+i}}, \quad (5)$$

$$UA = \frac{c_{ii}}{c_{i+}}, \quad (6)$$

$$OA = \sum_{i=1}^n \frac{c_{ii}}{N}, \quad (7)$$

where c_{ii} represents the number of pixels in row i and column i , c_{+i} represents the total sum of the i -th class in the ground truth pixels, c_{i+} represents the total sum of the i -th class in the classification result, N represents the total number of pixels, and n represents the total number of land cover classes.

3 Results

3.1 Feature selection results

To study the impact of feature quantity on model accuracy and select the best feature combination, the RFECV method is used for feature selection for each model. Figure 3 shows the curve of cross-validated scores as the number of features changes, based on RFECV feature selection applied to the original 20-dimensional features. The RF+RFECV line chart indicates that the model score is optimal when the number of features is 8 (RF_8). The feature combination at this point is B1, B5, B6, B9, B11, B12, MNDWI, and component_1_GLCMVariance. The LightGBM+RFECV line chart indicates that the model score is optimal when the number of features is 8 (LGBM_8). The feature combination at this point is B1, B5, B6, B9, B11, B12, MNDWI, and component_1_GLCMVariance. The XGBoost+RFECV line chart indicates that the model score is optimal when the number of

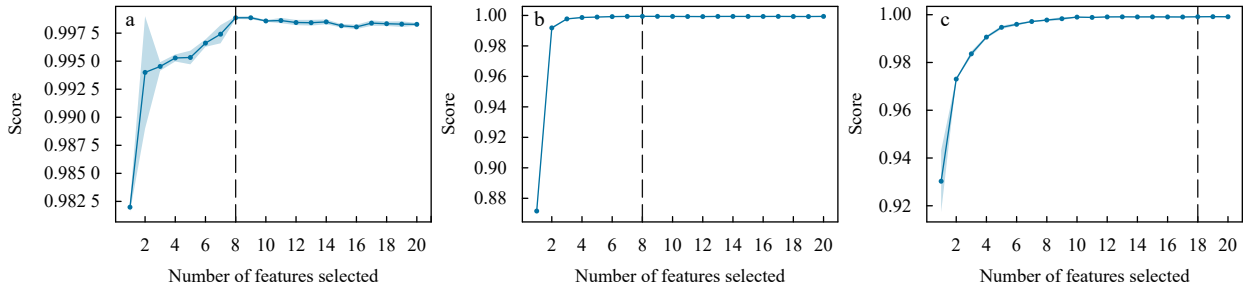


Fig. 3. Curve of cross-validated scores as the number of features changes, based on RFECV feature selection applied to the original 20-dimensional features. A line chart of RF+RFECV (a), a line chart of LightGBM+RFECV (b), and a line chart of XGBoost+RFECV (c) are shown on the top. The blue shading represents the fluctuation range.

features is 19 (XGB_19). The feature combination at this point is NDVI, MNDWI, RVI, DVI, B1, B2, B3, B4, B5, B6, B7, B8A, B9, B11, B12, component_1_Contrast, component_1_ASM, component_1_Entropy, and component_1_GLCMVariance.

Figure 4a displays the feature importance of the RF model and the overall model accuracy as the feature combination changes. The results show that as the number of features in the classification increases, the overall model accuracy also improves. However, after the inclusion of the fourth most important feature, B12, the overall model accuracy reaches nearly 1, and subsequent feature additions have little impact on the overall model accuracy. Additionally, it can be observed that the features component_1_GLCMVariance, B9, B11, B12, and B1 contribute more significantly to the improvement in overall model accuracy compared to other features.

Figure 4b shows the variation of *Spartina alterniflora* classification accuracy with different feature combinations. The results indicate that as the number of features

increases, the classification accuracy of *Spartina alterniflora* also improves. However, after the inclusion of the fourth feature, B12, there is no significant improvement in classification accuracy, similar to the overall trend of model accuracy with changing feature combinations. It is also evident that the four features: component_1_GLCMVariance, B9, B11, and B12, notably contribute to the improvement in *Spartina alterniflora* classification accuracy.

B11 and B12 belong to the SWIR range. In the September remote sensing images, the reflectance of *Spartina alterniflora* in the SWIR bands is significantly lower than that of other salt marsh vegetation such as reeds. These two bands can be used to distinguish *Spartina alterniflora* from other salt marsh vegetation. B9 belongs to the water vapor band, which is primarily used to detect the water vapor content in the atmosphere. In wetland environments, the water vapor content is relatively high, and the B9 band can effectively reflect this characteristic, thus helping to distinguish wetlands from other land cover types. The component_1_GLCMVariance tex-

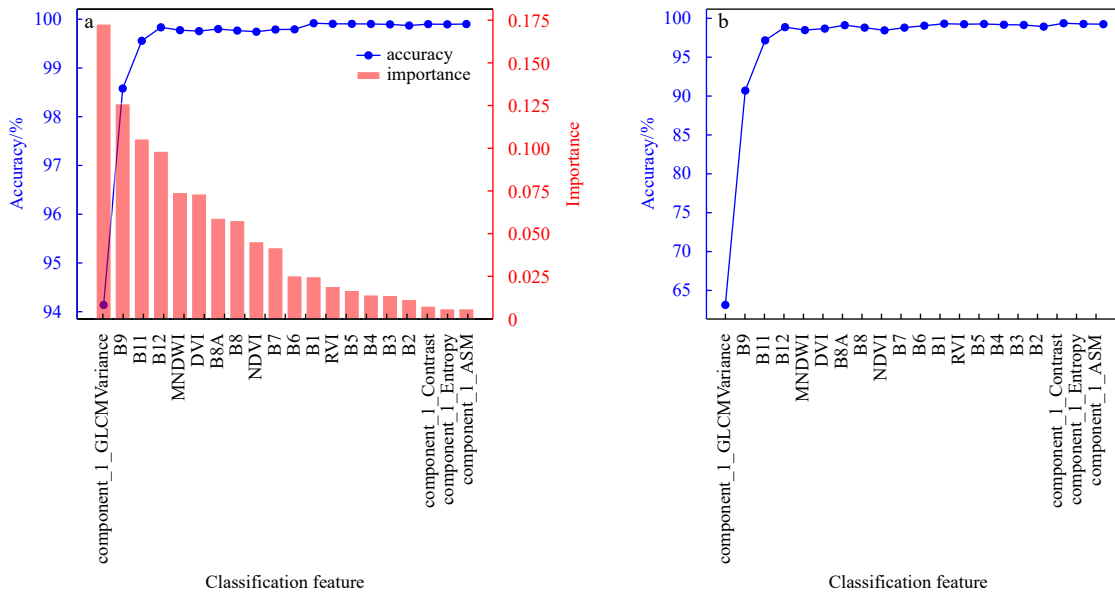


Fig. 4. Model accuracy with different features. a. Feature importance of the RF model and the overall model accuracy as the feature combination changes. b. Variation of *Spartina alterniflora* classification accuracy with different feature combinations. MNDWI: Modified Normalized Difference Water Index; NDVI: Normalized Difference Vegetation Index; RVI: Radar Vegetation Index.

ture feature has a stronger discriminative power for distinguishing between vegetation and non-vegetation compared to the other three texture features: component_1_Contrast, component_1_ASM, and component_1_Entropy. Although component_1_Contrast, component_1_ASM, and component_1_Entropy contain more information when observed from a grayscale image, they are too sensitive to changes in image grayscale. This sensitivity leads to less effective differentiation of various land cover types, including *Spartina alterniflora*.

Finally, based on the earlier RFECV analysis, we select B1, B5, B6, B9, B11, B12, MNDWI, and component_1_GLCMVariance as the final set of features to input into the model. Therefore, the combination of these eight features is called 8-feature combination.

3.2 Results of multi-model comparisons

The results (Fig. 5) indicate that the RF model performs better with the 8-feature combination than with the 20-feature combination, whereas XGBoost and LightGBM perform better with the 19-feature combination and 8-feature combination compared to the 20-feature combination. Overall, there is a notable improvement from the RF model with 20-feature combination to the RF model with 8-feature combination.

Table 3 shows the classification accuracy of wetland features in the experimental area by using different algo-

rithms, indicating that several models achieve similar classification accuracies. RF_8 shows a 0.03% increase in OA compared to RF_20, while LightGBM does not show a significant improvement, and XGB's OA decreases by 0.02%. This suggests that feature selection has a positive effect on RF. In terms of producer accuracy, the classification accuracy of RF_8 for reeds and *Spartina alterniflora* improved by 0.28% and 0.13% respectively, compared to before dimensionality reduction, while XGB_19's classification accuracy for *Spartina alterniflora* improved by 0.12% compared to XGB_20, but its classification accuracy for other land cover types was lower than XGB_20. LGBM_8's classification accuracy for farmland and the *Spartina alterniflora*-reed mixed transition zone improved by 0.05% and 0.05% respectively, compared to LGBM_20. RF_8's classification accuracy for reeds and the *Spartina alterniflora*-reed mixed transition zone was better than XGB_19, and its classification accuracy for the *Spartina alterniflora*-reed mixed transition zone was better than LGBM_8. However, LGBM_8's classification accuracy for *Spartina alterniflora* was 0.15% higher than RF_8, and its classification accuracy for farmland, reeds, and the *Spartina alterniflora*-reed mixed transition zone was better than XGB_19 by 0.05%, 0.01%, and 0.01% respectively. XGB_19's classification accuracy for *Spartina alterniflora* was 0.06% higher than LGBM_8. The results indicate that feature selection for

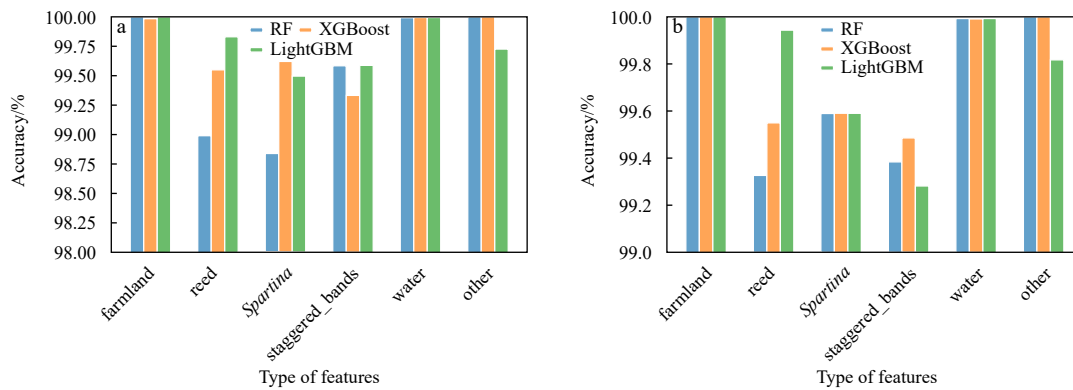


Fig. 5. Accuracy of various land covers under different models. a. Comparison of different models under 20 feature combinations. b. Comparison of optimal models. RF: Random Forest; XGBoost: eXtreme Gradient Boosting; LightGBM: Light Gradient Boosting Machine.

Table 3. Classification accuracy of wetland features in the experimental area using different algorithms

Type	RF_20		RF_8		XGB_20		XGB_19		LGBM_20		LGBM_8	
	PA/%	UA/%	PA/%	UA/%	PA/%	UA/%	PA/%	UA/%	PA/%	UA/%	PA/%	UA/%
Farmland	99.97	100.00	99.95	100.00	99.97	99.98	99.95	100.00	99.95	99.98	100.00	100.00
Reed	99.49	98.99	99.77	99.33	99.77	99.55	99.71	99.54	99.72	99.83	99.72	99.94
<i>Spartina alterniflora</i>	99.37	98.84	99.50	99.59	99.59	99.62	99.71	99.59	99.75	99.50	99.65	99.59
Staggered bands	98.26	99.58	99.23	99.38	99.23	99.33	99.17	99.48	99.13	99.59	99.18	99.28
Water	100.00	99.99	99.99	99.99	99.99	99.99	99.99	99.99	100.00	99.99	100.00	99.99
Other	100.00	100.00	100.00	100.00	100.00	100.00	100.00	100.00	100.00	99.73	100.00	99.81

Note: Staggered stands for *Spartina alterniflora*-reed mixed staggered zone; type stands for land cover type. PA stands for producer's accuracy; UA stands for user's accuracy. The overall accuracy values for RF_20, RF_8, XGB_20, XGB_19, LGBM_20, and LGBM_8 are 99.91%, 99.94%, 99.95%, 99.95%, 99.95%, and 99.95%, respectively.

RF and LightGBM helps reduce model complexity, significantly enhance the detection accuracy of *Spartina alterniflora*. Additionally, the images below provide a more intuitive comparison of the classification accuracy of different models for various land cover types. Considering that the LightGBM algorithm consumes fewer computational resources than RF and that the LightGBM model runs faster than RF in practice, this study ultimately chooses the LGBM_8 model for subsequent multi-temporal image classification and analysis.

3.3 Multi-temporal classification results

Figure 6 shows the selected four Sentinel-2 images at different times and the land cover interpretation results. It is evident that the model's classification results in January and September are similar to the land cover interpretation results, able to differentiate between reeds and *Spartina alterniflora* fairly well with minimal salt-and-pepper noise. However, the land cover classification performance in April and June, especially in the coastal wetland areas, shows significant areas of misclassification and salt-and-pepper noise. The results indicate that in September, the southern area of Chongming East Beach wetland has a larger area covered by *Spartina alterniflora* compared to other times, and the mixed zone is narrower in the September image than in June, indicating stronger competitive ability of *Spartina alterniflora* in the study area in September compared to reeds. In contrast, in January and April, the southern area of Chongming East Beach wetland has a smaller area covered by *Spartina alterniflora*, suggesting stronger competitive ability of reeds in the study area during January and April.

Through supervised classification of remote sensing images of the study area, we estimated that the area of *Spartina alterniflora* in Chongming East Beach is approx-

imately 1 122.73 hectares, and the area of reeds is about 2 491.47 hectares. In 2011, the area of *Spartina alterniflora* in Chongming East Beach had reached 13 000 hectares (Tang, 2016), severely encroaching on the distribution areas of many native species.

4 Discussion

To address the issue of the model's lack of interpretability, this study uses SHAP to conduct interpretability analysis of the model results. SHAP, a method proposed by Lundberg and Lee (2017) for explaining machine learning model predictions, is based on the Shapley value concept from game theory and considers each feature's contribution to the prediction outcome, providing an importance measure relative to a baseline value. SHAP constructs an additive explanation model where all features are considered "contributors". For each prediction sample, the model generates a prediction value, and the SHAP value represents the numerical contribution of each feature in that sample (Lundberg et al., 2020). Using SHAP to explain the results of machine learning models allows us to understand the relative importance of each feature for predictions. It helps us identify which features in the model have a more significant impact on the prediction results, enabling us to uncover the weaknesses and limitations of the model.

Figure 7 shows the SHAP summary plot for each land cover type. The SHAP summary plot illustrates the overall impact distribution of each feature on the model output. From Figs 7a–f, the land cover types are farmland, reed, *Spartina alterniflora*, staggered bands, water, and other. Red color represents high feature values, while blue color represents low feature values. The x -axis represents the magnitude of the SHAP values, where a point farther

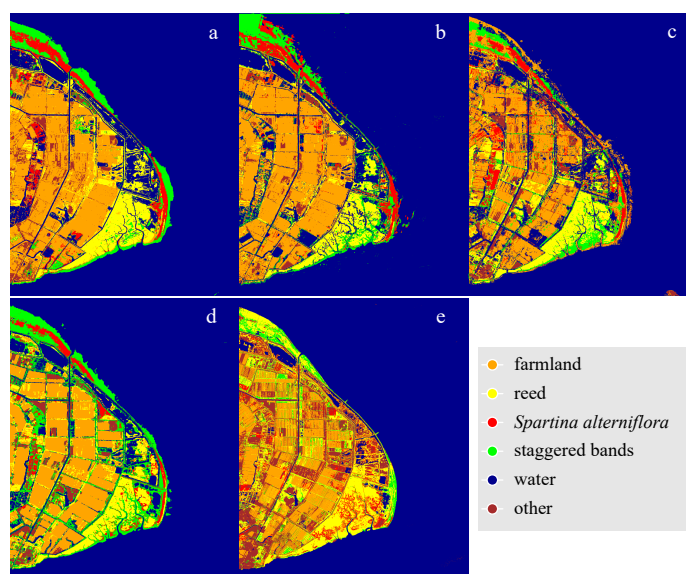


Fig. 6. Selected four Sentinel-2 images on January 21, 2020 (a), April 23, 2020 (b), June 2, 2020 (c), and September 5, 2020 (d), and the land cover interpretation results for land cover classification and *Spartina alterniflora* detection (e).

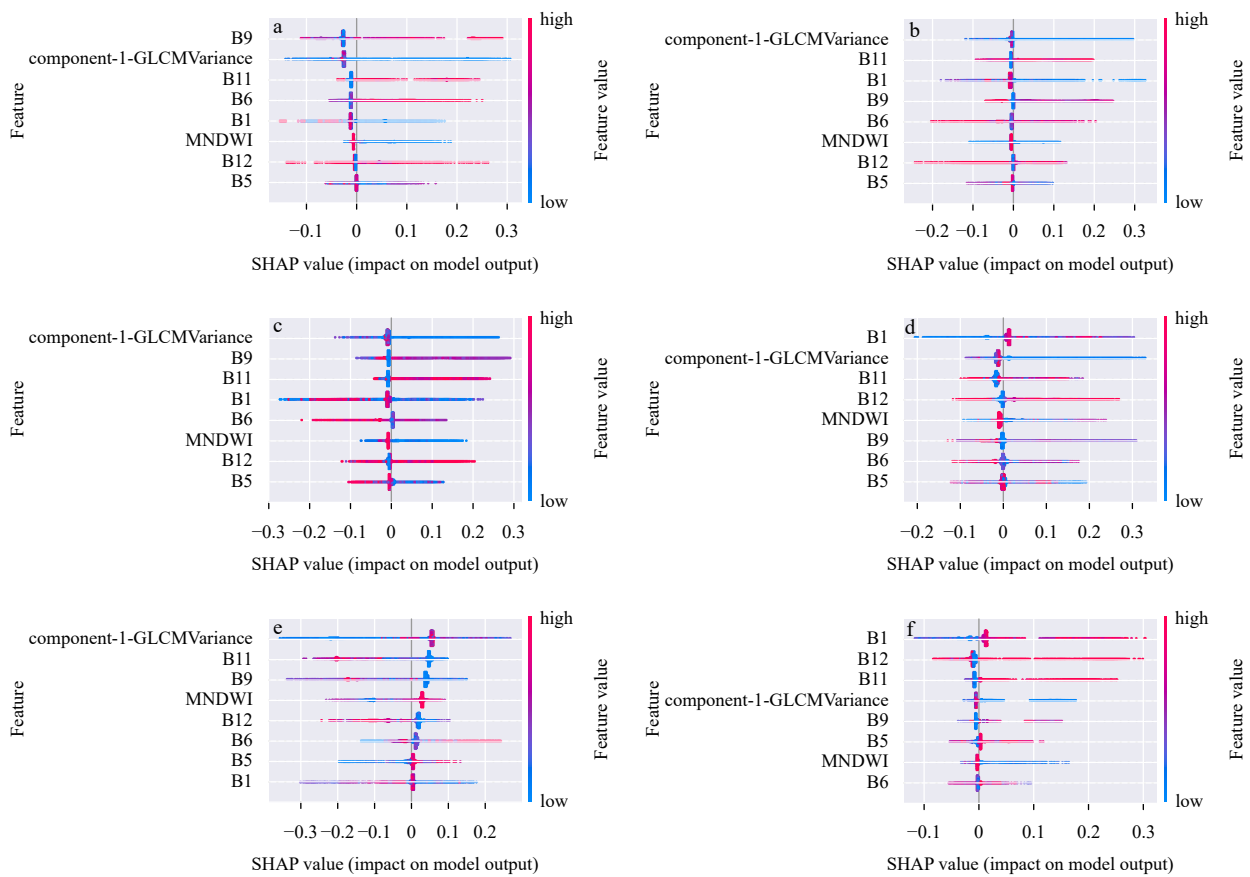


Fig. 7. SHapley Additive exPlanations (SHAP). Summary plot for each land cover type. a. SHAP summary plot for farmland classification, b. SHAP summary plot for breed classification, c. SHAP summary plot for *Spartina alterniflora* classification, d. SHAP summary plot for staggered bands classification, e. SHAP summary plot for water classification, and f. SHAP summary plot for other classification. Red color represents high feature values, while blue color represents low feature values. The x -axis represents the magnitude of the SHAP values, where a point farther from the zero baseline SHAP value indicates a stronger impact on the output. The left y -axis represents features, ranked in order of SHAP importance from top to bottom.

from the zero baseline SHAP value indicates a stronger impact on the output. The left y -axis represents features, ranked in order of SHAP importance from top to bottom. For example, in Fig. 7c, the features component_1_GLCMVariance, B9, and B11 are identified as important features influencing the accuracy of *Spartina alterniflora* classification. Specifically, when a pixel's component_1_GLCMVariance value is higher, the model is more likely to classify it as non-*Spartina alterniflora*. Conversely, when a pixel's B11 value is higher, the model is more likely to classify it as *Spartina alterniflora*.

From Figs 7a–d, it is also evident that the shortwave infrared bands B11 and B12 have a significant impact on vegetation classification accuracy. Overall, the feature component_1_GLCMVariance has a substantial influence on the accuracy of land cover classification across all types.

5 Conclusions

Satellite images enable large-scale and long-term observation of coastal objects such as *Spartina alterniflora*, and the algorithms based on deep learning require large

datasets with high computational power and poor interpretability. To solve the problem, a method is presented that starts from statistical learning and selects more comprehensive indicators (statistical features of GLCM+vegetation index+original spectral features) to choose a tree model that is more suitable for structured data with smaller computational complexity. This study utilizes RFECV feature selection and multi-model comparisons, leveraging multi-temporal Sentinel-2 imagery for supervised classification and *Spartina alterniflora* extraction. A model interpretation and visualization based on SHAP values were employed to explain the model results. The selected model and feature combination are effective in classifying land cover types in the study area and in identifying and detecting *Spartina alterniflora*.

Previous studies have used single or multi-temporal remote sensing images for wetland vegetation identification and mapping, and most of these studies employed original spectral information and related vegetation indices combined with machine learning or deep learning methods for wetland vegetation classification. This study integrates image texture features, vegetation indices, and raw spectral information, and uses multiple

models to detect and extract *Spartina alterniflora* in wetlands. It is found that image texture features significantly improve the accuracy of wetland vegetation classification and *Spartina alterniflora* identification. Additionally, the phenological characteristics of wetland vegetation are strong and diverse; effectively utilizing these phenological characteristics is highly beneficial for classification and monitoring of *Spartina alterniflora*. Besides, traditional machine learning models are often considered as “black box models” with poor interpretability. And it was shown that introducing SHAP helps us understand how models make decisions and address this interpretability issue. In the future, more experimental data and satellite images in different areas will be used to evaluate the method.

References

- Chen Xuewen, Jeong J C. 2007. Enhanced recursive feature elimination. In: Sixth International Conference on Machine Learning and Applications (ICMLA 2007). Cincinnati: IEEE, 429–435
- Costanza R, d'Arge R, De Groot R, et al. 1997. The value of the world's ecosystem services and natural capital. *Nature*, 387(6630): 253–260, doi: [10.1038/387253a0](https://doi.org/10.1038/387253a0)
- Cui Bin'ge, Wu Jing, Li Xinhui, et al. 2023. Combination of deep learning and vegetation index for coastal wetland mapping using GF-2 remote sensing images. *National Remote Sensing Bulletin (in Chinese)*, 27(6): 1376–1386, doi: [10.11834/jrs.20221658](https://doi.org/10.11834/jrs.20221658)
- Ding Wenhui, Jiang Junyan, Li Xiuzhen, et al. 2015. Spatial distribution of species and influencing factors across salt marsh in southern Chongming Dongtan. *Chinese Journal of Plant Ecology (in Chinese)*, 39(7): 704–716, doi: [10.17521/cjpe.2015.0067](https://doi.org/10.17521/cjpe.2015.0067)
- Feng Kaidong, Mao Dehua, Qiu Zhiqiang, et al. 2022. Can time-series sentinel images be used to properly identify wetland plant communities?. *GIScience & Remote Sensing*, 59(1): 2202–2216
- Gao Zhiqiang, Ai Jinquan, Gao Wei, et al. 2016. Integrating pan-sharpening and classifier ensemble techniques to map an invasive plant (*Spartina alterniflora*) in an estuarine wetland using Landsat 8 imagery. *Journal of Applied Remote Sensing*, 10(2): 026001, doi: [10.1117/1.JRS.10.026001](https://doi.org/10.1117/1.JRS.10.026001)
- Grinsztajn L, Oyallon E, Varoquaux G. 2022. Why do tree-based models still outperform deep learning on typical tabular data?. In: Proceedings of the 36th International Conference on Neural Information Processing Systems. New Orleans: Curran Associates Inc., 507–520
- Hall-Beyer M. 2017. Practical guidelines for choosing GLCM textures to use in landscape classification tasks over a range of moderate spatial scales. *International Journal of Remote Sensing*, 38(5): 1312–1338, doi: [10.1080/01431161.2016.1278314](https://doi.org/10.1080/01431161.2016.1278314)
- Jiang Lifen, Luo Yiqi, Chen Jiakuan, et al. 2009. Ecophysiological characteristics of invasive *Spartina alterniflora* and native species in salt marshes of Yangtze River estuary, China. *Estuarine, Coastal and Shelf Science*, 81 (1): 74–82
- Lan Zeyang, Liu Yang. 2018. Study on multi-scale window determination for GLCM texture description in high-resolution remote sensing image geo-analysis supported by GIS and domain knowledge. *ISPRS International Journal of Geo-Information*, 7(5): 175, doi: [10.3390/ijgi7050175](https://doi.org/10.3390/ijgi7050175)
- Lundberg S M, Erion G, Chen H, et al. 2020. From local explanations to global understanding with explainable AI for trees. *Nature Machine Intelligence*, 2(1): 56–67, doi: [10.1038/s42256-019-0138-9](https://doi.org/10.1038/s42256-019-0138-9)
- Lundberg S M, Lee S I. 2017. A unified approach to interpreting model predictions. In: Proceedings of the 31st International Conference on Neural Information Processing Systems. Long Beach: Curran Associates Inc., 4768–4777
- Mahdavi S, Salehi B, Granger J, et al. 2018. Remote sensing for wetland classification: A comprehensive review. *GIScience & Remote Sensing*, 55(5): 623–658
- Meng Xiangzhen, Liu Dan, Huang Ke, et al. 2021. Extraction method of *Spartina alterniflora* based on vegetation phenology characteristics: a case study of wetlands in the Changjiang River Delta. *Marine Science Bulletin (in Chinese)*, 40(5): 591–600
- Ouyang Zutao, Gao Yu, Xie Xiao, et al. 2013. Spectral discrimination of the invasive plant *Spartina alterniflora* at multiple phenological stages in a saltmarsh wetland. *PLoS ONE*, 8(6): e67315, doi: [10.1371/journal.pone.0067315](https://doi.org/10.1371/journal.pone.0067315)
- Ren Guangbo, Liu Yanfen, Ma Yi, et al. 2014. *Spartina alterniflora* monitoring and change analysis in Yellow River Delta by remote sensing technology. *Acta Laser Biology Sinica (in Chinese)*, 23(6): 596–603
- Segarra J, Buchaillet M L, Araus J L, et al. 2020. Remote sensing for precision agriculture: Sentinel-2 improved features and applications. *Agronomy*, 10(5): 641, doi: [10.3390/agronomy10050641](https://doi.org/10.3390/agronomy10050641)
- Shao Chunchen, Yang Gang, Sun Weiwei, et al. 2024. Construction method of a *Spartina alterniflora* index based on hyperspectral satellite images. *National Remote Sensing Bulletin (in Chinese)*, 28(3): 635–648, doi: [10.11834/jrs.20242621](https://doi.org/10.11834/jrs.20242621)
- Shu Minyan, Tian Bo, Ding Lixia, et al. 2019. Spectral analysis of an intertidal saltmarsh in the Yangtze Estuary. *Journal of Zhejiang A&F University (in Chinese)*, 36(1): 107–117
- Tang Chendong. 2016. Ecological control of *Spartina alterniflora* and improvement of birds habitats in Chongming Dongtan wetland, Shanghai. *Wetland Science & Management (in Chinese)*, 12(3): 4–8
- Xu Wei, Zhou Yunxuan, Shen Fang, et al. 2018. Recognition and extraction of *Phragmites australis* salt marsh vegetation in Chongming tidal flat from Sentinel-1A SAR data. *Journal of Jilin University (Earth Science Edition) (in Chinese)*, 48(4): 1192–1200
- Yao Hongyan, Liu Pudong, Shi Runhe, et al. 2017. Extracting the transitional zone of *Spartina alterniflora* and *Phragmites australis* in the wetland using high-resolution remotely sensed images. *Journal of Geo-Information Science (in Chinese)*, 19(10): 1375–1381
- Zhang Xin, Cui Jintian, Wang Weisheng, et al. 2017. A study for texture feature extraction of high-resolution satellite

- images based on a direction measure and gray level co-occurrence matrix fusion algorithm. *Sensors*, 17(7): 1474, doi: [10.3390/s17071474](https://doi.org/10.3390/s17071474)
- Zhang Siqing, Liu Yi, Liu Yiran, et al. 2021. Cellular automata simulation of population expansion dynamics of *Spartina alterniflora* in the Yellow River Delta. *Journal of Beijing Normal University (Natural Science)* (in Chinese), 57(1): 121–127
- Zhang Xi, Xiao Xiangming, Qiu Shiyun, et al. 2022. Quantifying latitudinal variation in land surface phenology of *Spartina alterniflora* saltmarshes across coastal wetlands in China by Landsat 7/8 and Sentinel-2 images. *Remote Sensing of Environment*, 269: 112810, doi: [10.1016/j.rse.2021.112810](https://doi.org/10.1016/j.rse.2021.112810)
- Zhu Yuling, Wang Jianbu, Wang Andong, et al. 2019. Remotesensed monitoring of *Spartina alterniflora* using deep convolutional neural network method with fusion of shallow features. *Marine Sciences* (in Chinese), 43(7): 12–22